Review Article

DIGITAL HEALTH

Digital Health
Volume 8: 1–12

DOI: 10.1177/20552076221111941
journals.sagepub.com/home/dhj
SAGE

An update on computational anthropomorphic anatomical models

Azadeh Akhavanallaf[1], Hadi Fayad[2,3], Yazdan Salimi[1], Antar Aly[2,3], Hassan Kharita[2], Huda Al Naemi[2,3] and Habib Zaidi[1,4,5,6]

Abstract

The prevalent availability of high-performance computing coupled with validated computerized simulation platforms as open-source packages have motivated progress in the development of realistic anthropomorphic computational models of the human anatomy. The main application of these advanced tools focused on imaging physics and computational internal/external radiation dosimetry research. This paper provides an updated review of state-of-the-art developments and recent advances in the design of sophisticated computational models of the human anatomy with a particular focus on their use in radiation dosimetry calculations. The consolidation of flexible and realistic computational models with biological data and accurate radiation transport modeling tools enables the capability to produce dosimetric data reflecting actual setup in clinical setting. These simulation methodologies and results are helpful resources for the medical physics and medical imaging communities and are expected to impact the fields of medical imaging and dosimetry calculations profoundly.

Keywords

Human anatomy, computational models, anthropomorphic models, Monte Carlo simulation, medical imaging

Submission date: 24 February 2022; Acceptance date: 19 June 2022

Introduction

Human anatomical models have been developed to represent the spatial distribution of different tissues in the body (human anatomy).[1,2] These models were mainly constructed to provide a non-invasive and inexpensive way to test various diagnostic imaging and interventional/therapeutic procedures,[3] such as dosimetric calculations for ionizing/non-ionizing radiation exposure, optimizing medical imaging facilities, and personalized medicine. An important category of anatomical models is physical phantoms composed of solid materials with properties equivalent to human tissues, e.g. homogenized cylindrical water phantoms used for the calibration of radiation detectors and diagnostic imaging systems.[4,5] However, these phantoms are usually expensive while reflecting a crude approximation of the human body. In addition, using physical phantoms for the calibration of advanced systems can be very costly and time-consuming. As a result, computational phantoms representing a mathematical model of the human anatomy in a digital format were developed originally for applications in radiation protection and medical imaging optimization. Recently, the ultimate objective of constructing human computational models as the ancestor of the digital twins (i.e. computational objects employed in medicine or other fields as surrogate or replica of the human body to certain process, e.g. to ionizing radiation) is the personalization

[1]Division of Nuclear Medicine and Molecular Imaging, Geneva University Hospital, Geneva, Switzerland
[2]Hamad Medical Corporation, Doha, Qatar
[3]Weill Cornell Medicine, Doha, Qatar
[4]Geneva University Neurocenter, Geneva University, Geneva, Switzerland
[5]Department of Nuclear Medicine and Molecular Imaging, University Medical Center Groningen, University of Groningen, Groningen, Netherlands
[6]Department of Nuclear Medicine, University of Southern Denmark, Odense, Denmark

Corresponding author:
Habib Zaidi, Division of Nuclear Medicine and Molecular Imaging, Geneva University Hospital, Geneva CH-1211, Switzerland.
Email: habib.zaidi@hcuge.ch

of medical procedures within the paradigm of precision medicine.[6] Starting in the 1960s, the development of the computational models evolved through many generations, and in the 1980s, further efforts were made in this domain. In this regard, the Visible Human Project led to the creation of the first complete anatomical model for dose calculation purposes.[7] The first generation of computational phantoms suffered from a variety of limitations, including lack of anatomical realism, the non-inclusion of tissue characteristics, calculation speed, as well as their incompatibility with available analytical or Monte Carlo simulation codes. More importantly, these computational phantoms have not been designed for subject-specific modeling and ignored inter-subject anatomical variability.[8]

Advances in high-performance computing stimulated the development and usage in research of realistic computational anthropomorphic models. To date, more than 200 computational phantoms have been reported in the literature.[2] Examples of widely used anatomical models are the NURBS-based XCAT phantom series[9] and the Virtual Population based on triangle mesh.[10,11] Advances in medical imaging modalities and computational algorithms allow fast construction of personalized computational models through automated segmentation techniques and enable the incorporation of physiological motion into anatomical models.

The fundamentals of computational models design

Multiple factors should be considered during the construction of a realistic anthropomorphic anatomical model.[12] These include anatomy (tissues, organs, and regions), tissue properties, computational efficiency, as well as compatibility with analytical or Monte Carlo simulation codes.

As a result, the first step in anthropomorphic anatomical model construction consists of defining geometrical surfaces and tissue properties. This can be done either by using constructive solid geometry (CSG) or boundary representation (BREP) approaches.[13,14] In CSG, objects are created using primitives, such as cylinders, ellipsoids, spheres, … etc. A number of examples can be found in the literature that fall under this category ranging from whole organ representation[8] to voxel-based representations.[15] Although whole organ representation approaches have the advantage that they are computationally efficient and compatible with existing Monte Carlo radiation transport simulation codes, they suffer from the lack of anatomical realism. Conversely, voxel-based representation has the advantage of reflecting anatomical realism that can be integrated into simulation codes.[15] However, the geometric fidelity is dependent on voxel size, and the simulations are computationally inefficient, especially for organ shapes readjustment. In BREP modeling, tissues can be characterized using boundary surfaces, such as non-uniform rational B-splines (NURBS) or polygon mesh surfaces. As in the case of voxel-based CSG, the data can be extracted from CT images by contouring organ surfaces followed by modeling to end up with smooth and continuous boundaries. The BREP representation better reflects anatomical realism compared to CSG, given that it can model complex anatomical features using an extended set of operation tools.

Although BREP models provide improved realism compared to previous modeling techniques, the corresponding models are still static. Therefore, a number of additional parameters have to be included to mimic the reality. There are many reasons behind this as summarized by Neufeld et al.[12]:

-Slow changes in anatomy during treatment in radiotherapy,
-Inter-subject anatomical variability in anthropomorphic parameters, such as height, weight, age, BMI, … etc,
-Need to have personalized models reflecting specific patient's anatomy/physiology,
-Voluntary or involuntary motion of organs, such as respiratory/cardiac motion or bowel movement that may affect quantitative analysis or radiation therapy planning.

Much worthwhile research efforts have been carried out in previous studies to handle some of the above-referenced limitations. The Visible Korean male phantom[16] is a landmark example where morphing techniques have been developed in order to modify the volume and shape of static phantoms. The employed methods include physics-based approaches,[12] image registration techniques[17,18] and geometrical approaches.[11,19,20] Finally, organ motion modeling techniques were developed to consider patients' involuntary respiratory motion. This led to a new generation of 4D computational models (3D space + time) that became practical tools for simulation in medical imaging as well as in radiotherapy treatment for oncological applications. Examples include respiratory motion simulation using rigid or elastic transformations, as adopted in the popular 4-D XCAT phantom,[21] and deformable voxelized phantoms[22] using more sophisticated techniques, such as finite element algorithms.[23]

From mathematical to voxel-based to boundary representation models

Computational human phantoms have been developed to realistically model patients' anatomy and physiology, considering the geometry and structures of organs/tissues, material composition, temporal changes, such as respiratory/cardiac motions, fluid dynamics such as blood flow or contrast perfusion, … etc.[24] Computational phantoms have been extended from simple water-filled slabs and spheres to anthropomorphic models with a realistic representation of the anatomy and material composition. Computational models are typically classified into three

main categories: (a) stylized phantoms, (b) voxel phantoms, and (c) boundary representation phantoms (Figure 1).

The first generation of computational phantoms was constructed for radiation protection purposes in the 1960s. It was primarily composed of simple macrobodies, easily described based on quadratic equations, such as cuboids, cylinders, spheres, ellipsoids, … etc.[26] The first anthropomorphic stylized phantom developed by Fisher and Snyder comprised only three regions (skeleton, lungs, and remainder tissues).[27] Nine years later, they built an improved version of their phantom composed of main organs defined by simple geometric primitives.[28] Along with the technical developments of stylized phantoms, diversities in the target population according to age (from newborn to adult), gender (male/ female), and pregnancy gestation (fetus models)[29–31] were modeled. For a long time, mathematical models served as the de facto standard in radiation protection and dose management. Many upgraded versions of these phantoms have been constructed, such as Adam and Eva,[32] precise head and brain models,[33] bone and marrow,[34,35] gastrointestinal tract,[36] … etc. Furthermore, to cover anatomical diversities of patient/worker populations, a library of stylized phantoms with different statures has been devised.[37] 4D stylized phantoms representing organ motion were developed based on surface equations, such as superquadratics[38] and non-uniform rational B-splines (NURBS).[39] Mathematical models have the advantages of easy manipulation of shape and size adjustment or motion simulation.[40] However, this design lacks anatomical realism as the model represents only a crude approximation of organs' shape and position. In addition, the definition of heterogenous tissue composition in macrobodies is not possible.

Through the advent of tomographic medical imaging modalities, such as CT and MRI, the visualization of the human anatomy in three-dimensions was made feasible. Medical images consist of small elements called pixels in 2D and voxels in 3D representing tissue information. To construct a 3D computational phantom, a label is assigned to each voxel according to the anatomical region (i.e. liver, brain, bone, … etc.) and tissue characteristics (material composition and density) obtained from medical images (i.e. CT or MRI). The segmentation of organs and tissues from medical images is traditionally performed manually, a labor-intensive and time-consuming process. Although voxel phantoms provided significant anatomical realism compared to stylized models, they suffer from limitations attributed to the finite voxel resolution of structural images (in the order of millimeters) and the inherent nature of voxel element geometry (uneven steps). In fact, tomographic images are not capable of representing fine structures in micrometer dimensions, such as the skin, eye lens, and epithelial tissue in the digestive tract. As a result, the anatomical fidelity of the developed model depends on voxel size, and most existing voxel models involve some level of assumptions about the anatomical structures. Furthermore, CT images that are mostly used as reference structural images do not generally represent soft-tissue contrast and typically cover only part of the body (not total-body images).

A number of reference anthropomorphic voxel phantoms have been developed mostly based on CT images. These reference models were first developed for the adult male model and later extended to the adult female, pediatric, and pregnant phantoms. In the late 1980s, Zankl et al. constructed voxel computational models using CT images of healthy patients that eventually ended up in 12-phantoms family representing different ages, gender, and size.[41–43] In 1994, a head-torso voxel model, referred to as the VoxelMan was developed from CT images to support imaging physics research in nuclear medicine.[44] In 2000, the VIP-Man phantom was developed by Xu et al. as the first model constructed based on color photographic images of a cadaver.[45] In 2002, the dose Calculation task group of the International Commission on Radiological Protection (ICRP) Committee launched a project focusing on the development of a set of standard voxel phantoms to be released to the public as the ICRP reference phantoms (adult male and female).[46] Bolch et al. created a series of pediatric reference phantoms from newborn to 15-year-old teenager.[47] As the most recent developed pediatric family phantoms, ICRP publication 143 describes the development of a series of 10 computational models composed of male and female newborn, 1 year, 5 years, 10 years, and 15 years old phantoms.[48]

Computational models based on boundary representation techniques were introduced as a new computational model generation taking advantage of both mathematical and voxel-based models. BREP phantoms are able to represent realistic anatomy of the human body while benefiting from the advantages of mathematical phantoms in modeling the deformations. Surface-based models, such as non-uniform rational B-splines and polygon mesh models, are subcategories of BREP modeling. These advanced surface models are capable of realistically representing the anatomical structures while enabling the simulation of anatomical deformation (posture and involuntary organ motion) by providing a rich set of mathematical operation tools. In surface-based designs, the transformations can be simply applied to the surfaces or vertex points to morph the object.

In the BREP or hybrid approach, voxel data are combined with stylized modeling techniques to design a computational phantom that benefits the advantages of both voxel models in representing the anatomical realism and stylized phantoms in providing the flexibility for anatomical variations.[49] A series of reference phantoms (adult and pediatric) in hybrid format has been developed by the University of Florida.[50–52] A series of hybrid pregnant female phantoms at the end of three gestational periods has been developed

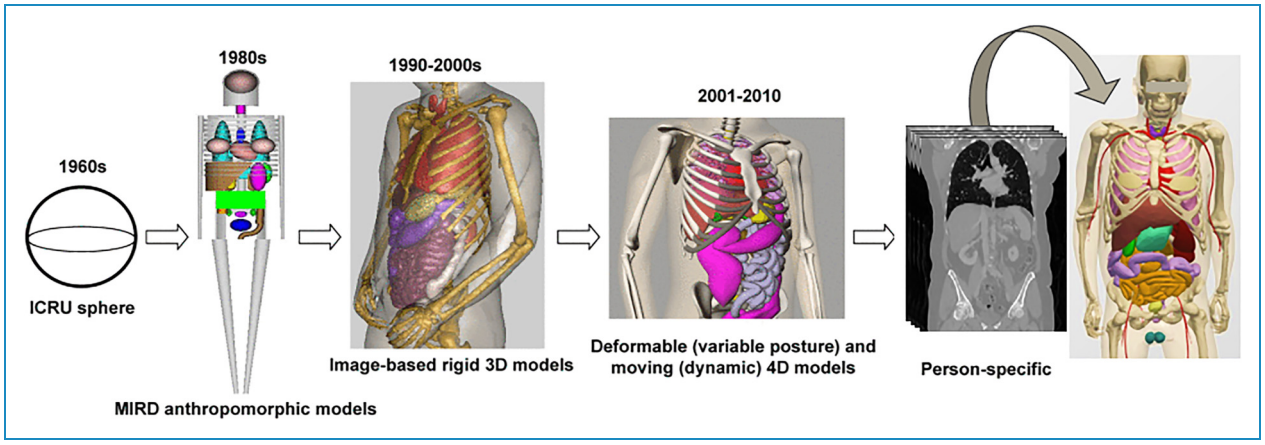

Figure 1. The evolution of computational phantoms from simple macro-bodies to detailed personalized models. Adapted with permission from.[25]

by Xu et al.,[53] whereas a family of Iranian BREP phantoms (adult male/female and pregnant reference phantoms) has been developed at Ferdowsi University of Mashhad[54–56] as illustrated in Figure 2. The Virtual Family, a series of surface-based computational phantoms, has been developed based on high-resolution MR images.[10,11] A polygon surface phantom at Hanyang University in Korea extended from the reference voxel model of VKH-Man was also designed.[57] Recently, mesh-type ICRP reference adult phantoms, which account for surface-based counterparts of the voxel-type ICRP reference phantoms, have also been developed.[58,59]

Extensions of reference phantoms

Motion and posture simulation

Reference computational phantoms are constructed using tomographic images of a single subject, thus lacking inter-subject anatomical variability. In addition, reference models have been traditionally developed as static models where the physiological dynamics of the human body behavior is ignored. To address these limitations, a library of anatomically variable computational phantoms and time-varying 4-D reference phantoms have been developed.

In digital models, physiological motion is typically captured from gated imaging, where the data acquisition is synchronized with a physiological signal. This information is used to simulate motion through time-varying transformations of the body structures. In BREP designed phantoms, the topological transformations are applied to surface control points. The 4-D NCAT phantom, an extension from the earlier mathematical MCAT phantom by Segars et al.,[39,60] representing cardiac and respiratory motions, was the first NURBS-based torso model. In an updated version, the 4-D XCAT phantom family was extended to include a series of 47 phantoms representing cardiac and respiratory motions of different patients.[61] A number of studies reported on the extension of 4D XCAT phantoms. For instance, Ghaly et al.[62] developed a population of 4D phantoms by deforming the 3D XCAT reference model. In addition, Konik et al.[63] simulated non-rigid respiratory and voluntary body motion based on the XCAT model. The 4-D VIP-Man phantom developed based on polygonal mesh was employed for occupationally incorporated radioactivity in the lung region.[64] For CSG design, respiratory motion transformations are applied to individual voxels by linear interpolation of the deformation vector fields to generate a series of high-temporal-resolution voxel phantoms.[22]

Morphing and changing the posture of reference phantoms is a useful technique to mimic real-world scenarios in the radiation protection domain.[2] Since building a new posture-specific phantom is challenging and time-consuming, morphing techniques have been developed enabling the deformation of volumetric and topological features of organs and structures from existing reference computational models. Strategies for morphing the anatomy encompass simple heuristic methods for scaling and transpositions of organs to complex non-rigid registration techniques.[19,65] These strategies were exploited to extend a series of computational phantoms with different anatomical characteristics, such as height, weight, BMI, … etc., from a reference computational model. This strategy will be further elaborated in the section below "Libraries of computational human phantoms." To simulate physiological motion of anatomical structures, posture-specific phantoms have been devised. The postures were adjusted based on the information derived from a body motion capture system to realistically simulate sequence of body movements.[20,66] Han et al.[67] developed walking phantoms suitable for radiation dosimetry in external photon exposure scenarios. Another study by Su et al.[68] reported on sitting phantoms designed for internal radiation dosimetry studies.

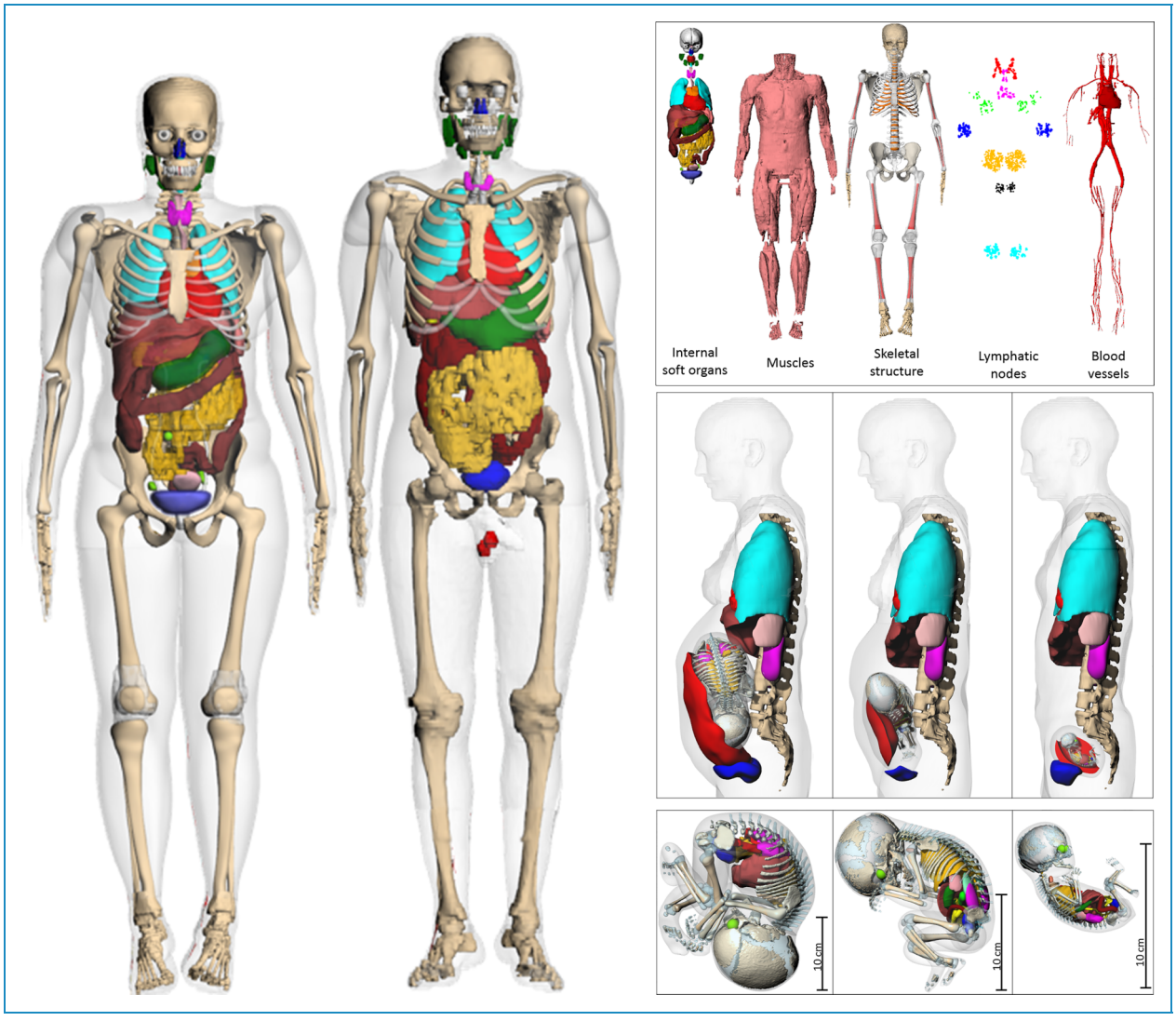

Figure 2. The reference BREP Iranian computational phantoms. Left panel: Male/female adult reference computational phantoms. Right-top panel: The segmented structural/anatomical details and, Right-bottom panel: The reference pregnant phantom with fetus model at three gestation periods. Courtesy of Dr Miri and Dr Rafat, Ferdowsi University of Mashhad.

Recently, mesh-type ICRP phantoms were deformed to multiple non-standing postures using a posture-change method based on a rigid shape-deformation algorithm and motion-capture technology[69] to measure the radiation dose in specific situations.

Libraries of computational human phantoms

Reference phantoms are constructed according to the anatomical characteristics of a single subject considering anthropomorphic data of the average population, therefore lacking inter-subject anatomical variability. The diversity of anthropometric parameters between individuals raises the demand for building patient-specific computational phantoms. Although personalized phantoms are deemed to represent the ideal digital twins, there are some limitations associated with the construction of individualized phantoms. This includes the lack of high-resolution tomographic images for specific patients and the time-consuming procedures for organ/tissue segmentation. In this regard, habitus-specific phantom series created based upon the deformation of a reference phantom assembling different anatomical variables for population-based assessments have been introduced. Deformation algorithms have been typically developed based on morphing the tissues considering hyper-elastic soft-tissue and stiff joints. Some interactive tools enabling topological morphing and interpolation of tissues, such as tissue growth (analogous to thermal expansion), to construct a habitus-variable computational population from a reference model have been

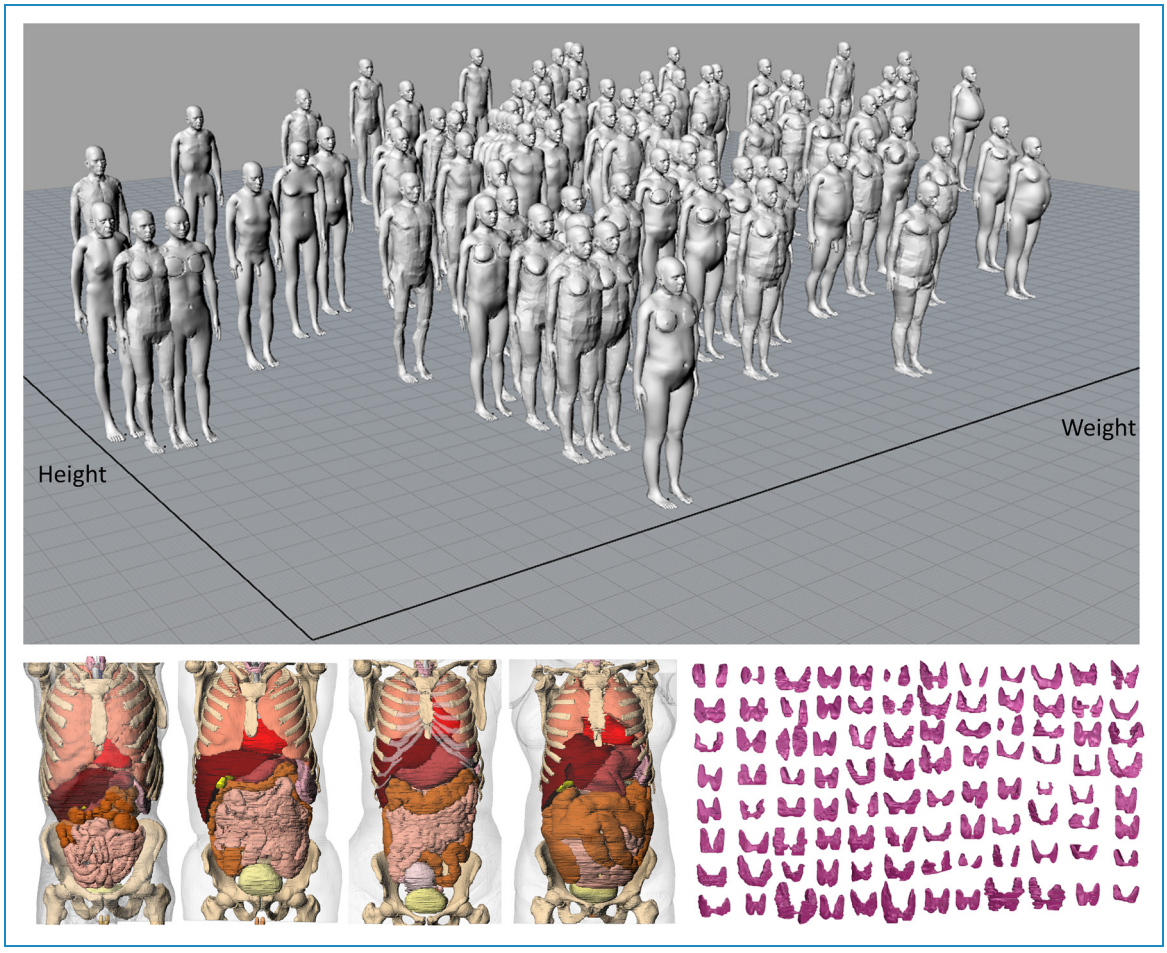

Figure 3. Series of adult computational phantoms (males and females) developed based on CT images of healthy Iranian population. The distribution of anthropomorphic indices, height and weight (top panel), along with the structural details of the developed computational models (left-bottom panel) are shown. As an example, the anatomical deviations of the thyroid gland in this population is illustrated (right-bottom panel). Courtesy of Dr Miri and Dr Rafat, Ferdowsi University of Iran.

developed. A number of studies reported on size-adjustable phantoms representing the variability of anatomical and anthropomorphic parameters, such as body size, organ volume/shape, … etc. Johnson et al.[70] extended the UF hybrid adult phantoms to 25 habitus-specific computational phantoms. Na et al.[19] reported on the construction of a library of adult phantoms (weight-specific) extended from the RPI reference models using an automated deformation algorithm implemented on polygon mesh surfaces. In addition, a number of obese phantoms and a set of age-dependent Chinese computational models in mesh format have been developed based on the RPI reference phantoms to examine the effect of obesity on CT dosimetry.[71,72] Broggio et al.[73] constructed 25 adult phantoms to cover the diversity of heights and weights in the adult male population. Lloyd et al.[74] developed a non-rigid deformation algorithm to extend the population of the Virtual Family phantoms using biomechanical finite element methods. Geyer et al.[75] extended the UF phantom family to height/weight-specific phantoms. A Korean library of voxel phantoms has been developed to represent different body shapes and sizes.[76] More recently, Akhavanallaf et al.[65] developed an automated algorithm to construct a comprehensive library of phantoms extended from voxel-based ICRP reference phantoms. Choi et al.[77] extended a body-size dependent family of adult phantoms based on mesh-type ICRP reference phantoms. Hoseinian et al.[78–80] created a comprehensive series of BREP whole-body phantoms covering statistical diversities of the Iranian population (Figure 3). Beside the development of total-body phantom families, Erickson et al.[81] established a database of realistic virtual breast models based on breast computed tomography images.

Advances in computational models

Recent advances in computational phantoms design focused on two main aspects: first, realistic representation

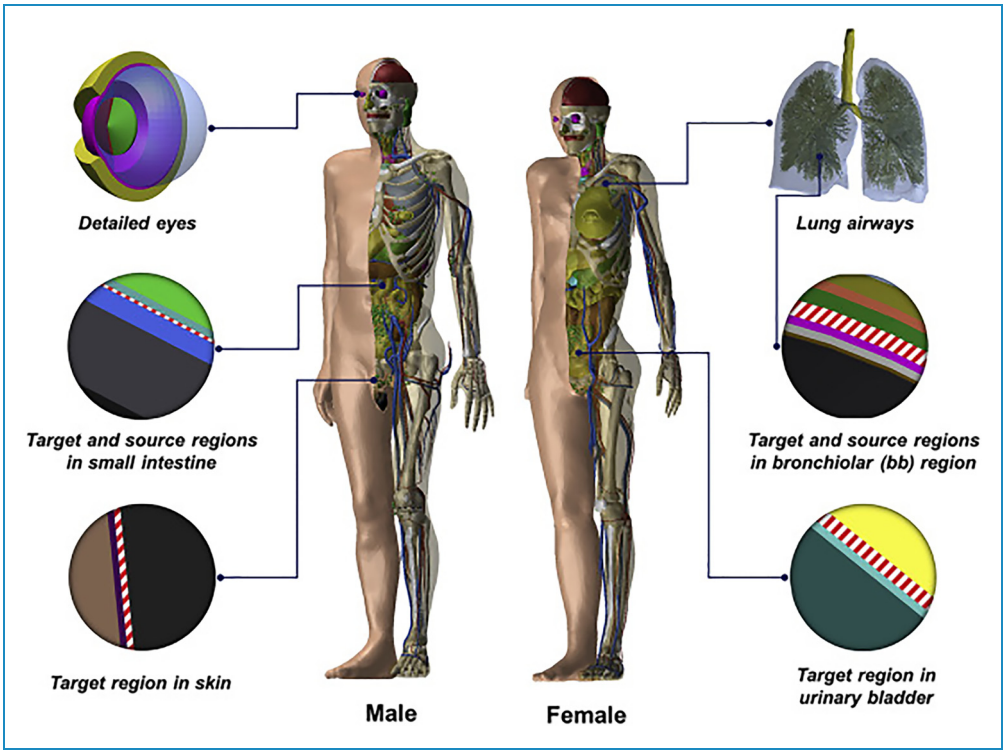

Figure 4. Adult male and female mesh-type ICRP reference computational phantoms. Micron-scale radiosensitive regions of major organs and tissues are visualized on the left and right sides of the phantoms. Reprinted with permission from.[88]

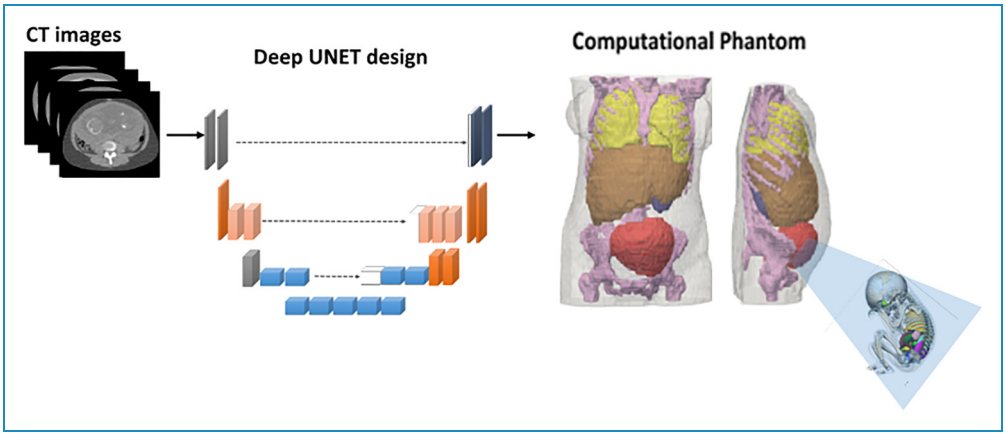

Figure 5. Illustration of the deep learning pipeline used to automatically generate pregnant computational phantoms.

of patient-specific anatomy; and second, upgrade of reference phantoms by adding small (micrometer-scale) or complex anatomical structures. The anatomical fidelity of the developed computational phantoms depends strongly on the voxel resolution of the reference tomographic images. Current imaging technologies are not capable of representing complex or fine structures, such as bone marrow, eye lens, alimentary tract structures, … etc., in micrometer-scale. In this context, Yeom et al. from Hanyang University developed mesh type ICRP phantoms extended from the reference ICRP voxel models through preserving the original anatomical structures. Complex structures of the gastrointestinal system have been improved and the fine structures of the alimentary and respiratory tracts and lung airways were added (Figure 4).[82,83] In a recent study, mesh-type skeletal systems for pediatric population and detailed eye models for children and adolescents of the ICRP reference phantoms were developed in a fine-structure.[84,85] Abadi et al.[86] elaborated on the lung architecture of the XCAT

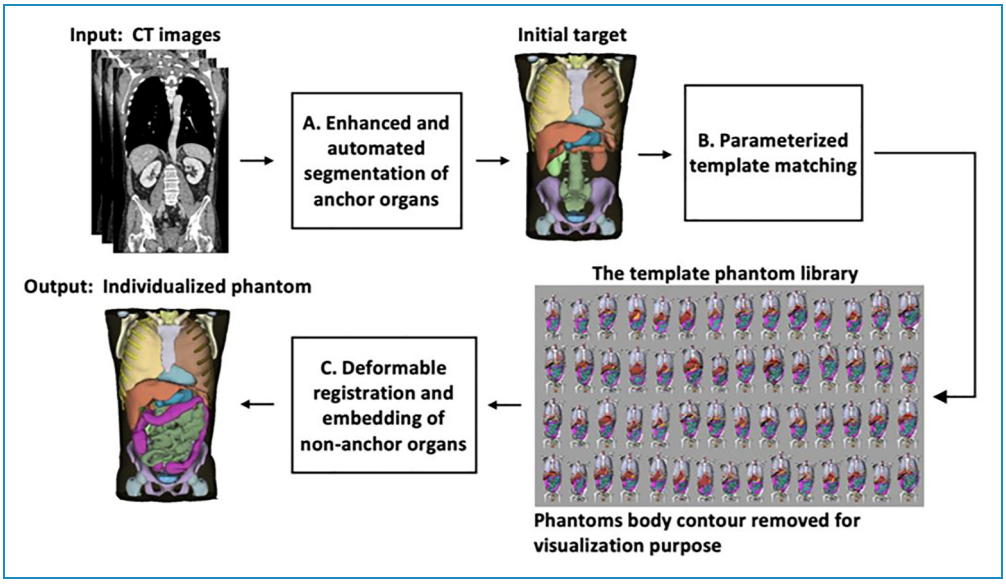

Figure 6. The pipeline for automated construction of personalized computational phantoms. Reprinted with permission from.[91]

series by modeling the airways and pulmonary vasculature. MIDA is a detailed head and neck model (over 160 structures) constructed from a series of high-resolution multimodal MR sequences.[87] In parallel, advanced functionalized anatomical models have been developed.[12]

Toward the 4th-generation patient-specific digital twins, semi-automatic segmentation techniques based on texture patterns or manual delineation along with deformable registration algorithms have been traditionally employed. In state-of-the-art approaches, this process was labor-intensive and time-consuming which limited the construction of patient-specific computational models.[89] Recently Carter et al. proposed to use deformable registration techniques to create individualized phantoms to better support patient-specific dosimetry.[90] Thanks to recent advances in artificial intelligence algorithms, fully automated segmentation of medical images became feasible. In this field, machine learning and deep learning techniques proved to serve as useful techniques to generate patient-specific phantoms. Deep learning algorithms demonstrated their capabilities in image segmentation[91–95] and image registration[91,96] that can be integrated into the workflow for the construction of patient-specific computational phantoms for diagnostic and radiotherapy risk assessment purposes.[97,98] In 2019, Xie et al.[99] constructed patient-specific pregnant phantoms by means of deep learning anchor organ segmentation and used them as input for Monte Carlo organ dose calculations. As illustrated in Figure 5, the generated patient-specific phantoms were utilized to estimate fetal exposure from abdominal CT examinations.

Peng et al.[92] used deep learning techniques to automatically segment CT images and combined it with accelerated Monte Carlo simulations to calculate patient-specific radiation dose to make the implementation of the proposed approach in clinical setting feasible. They claimed that the proposed patient-specific phantom constructed based on automatic segmentation is prone to much less error compared with the selection of a computational phantom from available libraries. Recently Fu et al.[91] developed a unified pipeline to create personalized computational models from radiological images. The proposed pipeline is composed of three main steps: first, some anchor organs were segmented from CT images using deep learning algorithms; second, the best-matching reference phantom was selected from a template phantom library using parametrized template matching approach; and third, a deformable registration between CT images merged with anchor organ masks and the selected reference phantom was carried out. They registered patient images to one of the phantoms selected from the XCAT library (Figure 6).

Summary and future perspectives

Advances in high-performance computing and the capabilities offered by deep learning-based algorithms have triggered important developments toward the 4th generation of human computational models called digital twins which represent the biological and physical characteristics of the human body from gene information to anthropomorphic parameters. Recent advances in deep learning–assisted medical image analysis and processing successfully pushed the borders toward real-time patient-specific computational models. Considering the time-consuming process of organs labeling and generation of ground truth in the supervised approach, novel unsupervised models,

such as variational auto-encoders or generative adversarial networks, seem promising for application in this area.[100]

Acknowledgments: We acknowledge Dr Hashem Miri and Dr Lale Rafat at Ferdowsi University of Iran for providing illustrations of their computational models.

Author contributions: The authors provided have the entire authorship of this article. All authors read and approved the final manuscript.

Declaration of conflicting interests: The author(s) declared no potential conflicts of interest with respect to the research, authorship, and/or publication of this article.

Funding: The author(s) disclosed receipt of the following financial support for the research, authorship, and/or publication of this article: This work was supported by the Qatar national research fund (grant number NPRP10-0126-170263) and the Swiss National Science Foundation under grant SNRF 320030_176052.

Ethical approval: Not applicable, because this article does not contain any studies with human or animal subjects.

Informed consent: Not applicable, because this article does not contain any studies with human or animal subjects.

ORCID iDs: Antar Aly https://orcid.org/0000-0002-2325-6610
Habib Zaidi https://orcid.org/0000-0001-7559-5297

Trial registration: Not applicable, because this article does not contain any clinical trials.

Guarantor: HZ

References

1. Caon M. Voxel-based computational models of real human anatomy: a review [published online ahead of print 2004/01/20]. *Radiat Environ Biophys* 2004; 42: 229–235.
2. Kainz W, Neufeld E, Bolch WE, et al. Advances in computational human phantoms and their applications in biomedical engineering – a topical review [published online ahead of print 2019/02/12]. *IEEE Trans Radiat Plasma Med Sci* 2019; 3: 1–23.
3. Zaidi H and Xu XG. Computational anthropomorphic models of the human anatomy: the path to realistic Monte Carlo modeling in radiological sciences [published online ahead of print 2007/02/15]. *Annu Rev Biomed Eng* 2007; 9: 471–500.
4. Tajik M, Akhlaqi MM and Gholami S. Advances in anthropomorphic thorax phantoms for radiotherapy: a review [published online ahead of print 20211104]. *Biomed Phys Eng Express* 2021. DOI: 10.1088/2057-1976/ac369c.
5. Filippou V and Tsoumpas C. Recent advances on the development of phantoms using 3D printing for imaging with CT, MRI, PET, SPECT, and ultrasound [published online ahead of print 20180622]. *Med Phys* 2018; 45: e740–e760.
6. Popa EO, van Hilten M, Oosterkamp E, et al. The use of digital twins in healthcare: socio-ethical benefits and socio-ethical risks [published online ahead of print 20210705]. *Life Sci Soc Policy* 2021; 17: 6.
7. Spitzer V, Ackerman MJ, Scherzinger AL, et al. The visible human male: a technical report [published online ahead of print 1996/03/01]. *J Am Med Inform Assoc* 1996; 3: 118–130.
8. Xu XG. An exponential growth of computational phantom research in radiation protection, imaging, and radiotherapy: a review of the fifty-year history [published online ahead of print 2014/08/22]. *Phys Med Biol* 2014; 59: R233–R302.
9. Segars WP, Tsui BMW, Jing C, et al. Application of the 4-D XCAT phantoms in biomedical imaging and beyond [published online ahead of print 2017/08/16]. *IEEE Trans Med Imaging* 2018; 37: 680–692.
10. Christ A, Kainz W, Hahn EG, et al. The virtual family--development of surface-based anatomical models of two adults and two children for dosimetric simulations [published online ahead of print 2009/12/19]. *Phys Med Biol* 2010; 55: N23–N38.
11. Gosselin MC, Neufeld E, Moser H, et al. Development of a new generation of high-resolution anatomical models for medical device evaluation: the Virtual Population 3.0 [published online ahead of print 2014/08/22]. *Phys Med Biol* 2014; 59: 5287–5303.
12. Neufeld E, Lloyd B, Schneider B, et al. Functionalized anatomical models for computational life sciences [published online ahead of print 2018/12/07]. *Front Physiol* 2018; 9: 1594.
13. Leyton M. *A generative theory of shape*. Vol. 2145. Heidelberg: Springer, 2003.
14. Stroud I. *Boundary representation modelling techniques*. London: Springer, 2006.
15. Schneider W, Bortfeld T and Schlegel W. Correlation between CT numbers and tissue parameters needed for Monte Carlo simulations of clinical dose distributions [published online ahead of print 2000/03/04]. *Phys Med Biol* 2000; 45: 459–478.
16. Park JS, Chung MS, Hwang SB, et al. Visible Korean human: improved serially sectioned images of the entire body [published online ahead of print 2005/03/10]. *IEEE Trans Med Imaging* 2005; 24: 352–360.
17. Segars WP, Norris H, Sturgeon GM, et al. The development of a population of 4D pediatric XCAT phantoms for imaging research and optimization [published online ahead of print 2015/08/04]. *Med Phys* 2015; 42: 4719–4726.
18. Akbarzadeh A, Gutierrez D, Baskin A, et al. Evaluation of whole-body MR to CT deformable image registration [published online ahead of print 2013/07/10]. *J Appl Clin Med Phys* 2013; 14: 4163.
19. Na YH, Zhang B, Zhang J, et al. Deformable adult human phantoms for radiation protection dosimetry: anthropometric data representing size distributions of adult worker populations and software algorithms [published online ahead of print 2010/06/17]. *Phys Med Biol* 2010; 55: 3789–3811.

20. Fonseca TC, Bogaerts R, Hunt J, et al. A methodology to develop computational phantoms with adjustable posture for WBC calibration [published online ahead of print 2014/10/22]. *Phys Med Biol* 2014; 59: 6811–6825.
21. Segars WP, Sturgeon G, Mendonca S, et al. 4D XCAT phantom for multimodality imaging research [published online ahead of print 2010/10/23]. *Med Phys* 2010; 37: 4902–4915.
22. Han MC, Seo JM, Lee SH, et al. Continuously deforming 4D voxel phantom for realistic representation of respiratory motion in Monte Carlo dose calculation. *IEEE Trans Nucl Sci* 2016; 63: 2918–2924.
23. Segars WP, Veress AI, Sturgeon GM, et al. Incorporation of the living heart model into the 4D XCAT phantom for cardiac imaging research [published online ahead of print 2019/02/16]. *IEEE Trans Radiat Plasma Med Sci* 2019; 3: 54–60.
24. Abadi E, Segars WP, Tsui BMW, et al. Virtual clinical trials in medical imaging: a review [published online ahead of print 2020/04/22]. *J Med Imaging (Bellingham)* 2020; 7: 042805.
25. Zaidi H and Tsui BMW. Review of computational anthropomorphic anatomical and physiological models. *Proc IEEE* 2009; 97: 1938–1953.
26. Fisher J and Snyder W. Variation of dose delivered by137 Cs as a function of body size from infancy to adulthood. *ORNL-4007*. 1966.221–228.
27. Snyder WS, Fisher HLJr, Ford MR, et al. Estimates of absorbed fractions for monoenergetic photon sources uniformly distributed in various organs of a heterogeneous phantom. *J Nucl Med* 1969(Suppl 3):7–52.
28. Snyder W, Ford M and Warner G. Estimates of specific absorbed fractions for photon sources uniformly distributed in various organs of a heterogeneous phantom 1978 Oak Ridge National Laboratory NM/MIRD Pamphlet No. 5. *Oak Ridge National Laboratory NM/MIRD Pamphlet.* 1978. (5).
29. Cristy M. *Mathematical phantoms representing children of various ages for use in estimates of internal dose*. TN, USA: Oak Ridge National Lab., 1980.
30. Stabin M, Watson E, Cristy M, et al. *Mathematical models and specific absorbed fractions of photon energy in the nonpregnant adult female and at the end of each trimester of pregnancy*. TN, USA: Oak Ridge National Lab., 1995.
31. Cristy M and Eckerman K. *Specific absorbed fractions of energy at various ages from internal photon sources: 1, methods*. TN, USA: Oak Ridge National Lab., 1987.
32. Kramer R, Zankl M and Williams G,GD. *The male (Adam) and female (Eva) adult mathematical phantoms*. Germany: GSF, 1986.
33. Bouchet LG, Bolch WE, Weber DA, et al. Mird pamphlet no. 15: radionuclide S values in a revised dosimetrie model of the adult head and brain. *J Nucl Med* 1999; 40: 62S–101S.
34. Eckerman KF and Stabin MG. Electron absorbed fractions and dose conversion factors for marrow and bone by skeletal regions [published online ahead of print 2000/01/27]. *Health Phys* 2000; 78: 199–214.
35. Bouchet LG, Bolch WE, Howell RW, et al. S values for radionuclides localized within the skeleton [published online ahead of print 2000/01/27]. *J Nucl Med* 2000; 41: 189–212.
36. Poston JWJr, Kodimer KA, Bolch WE, et al. A revised model for the calculation of absorbed energy in the gastrointestinal tract [published online ahead of print 1996/09/01]. *Health Phys* 1996;71:307–314.
37. Clairand I, Bouchet LG, Ricard M, et al. Improvement of internal dose calculations using mathematical models of different adult heights [published online ahead of print 2000/10/26]. *Phys Med Biol* 2000; 45: 2771–2785.
38. Peter J, Gilland D, Jaszczak R, et al. Four-dimensional superquadric-based cardiac phantom for Monte Carlo simulation of radiological imaging systems. *IEEE Trans Nucl Sci* 1999; 46: 2211–2217.
39. Segars WP. *Development and application of the new dynamic NURBS-based cardiac-torso (NCAT) phantom*. The University of North Carolina at Chapel Hill, 2001.
40. Pretorius PH, Xia W, King MA, et al. Evaluation of right and left ventricular volume and ejection fraction using a mathematical cardiac torso phantom [published online ahead of print 1997/10/23]. *J Nucl Med* 1997; 38: 1528–1535.
41. Williams G, Zankl M, Abmayr W, et al. The calculations of dose from external photon exposures using reference and realistic human phantoms and Monte Carlo methods [published online ahead of print 1986/04/01]. *Phys Med Biol* 1986; 31: 449–452.
42. Zankl M, Veit R, Williams G, et al. The construction of computer tomographic phantoms and their application in radiology and radiation protection [published online ahead of print 1988/01/01]. *Radiat Environ Biophys* 1988; 27: 153–164.
43. Zankl M, Becker J, Fill UA, et al. GSF Male and female adult voxel models representing ICRP reference man-the present status. In: Paper presented at: The Monte Carlo method: versatility unbounded in a dynamic computing world proc. of the Monte Carlo 2005 topical meeting on CD-ROM (Chattanooga, TN, 17–21 April 2005) (LaGrange, Park IL: American Nuclear Society), 2005.
44. Zubal IG, Harrell CR, Smith EO, et al. Computerized three-dimensional segmented human anatomy [published online ahead of print 1994/02/01]. *Med Phys* 1994; 21: 299–302.
45. Xu XG, Chao TC and Bozkurt A. VIP-Man: an image-based whole-body adult male model constructed from color photographs of the Visible Human Project for multi-particle Monte Carlo calculations. *Health Phys* 2000; 78: 476–486.
46. Menzel HG, Clement C and DeLuca PICRP. Adult reference computational phantoms. ICRP Publication 110. *Ann ICRP* 2009; 39: 1–164.
47. Lee C, Williams JL, Lee C, et al. The UF series of tomographic computational phantoms of pediatric patients [published online ahead of print 2006/02/16]. *Med Phys* 2005; 32: 3537–3548.
48. Bolch WE, Eckerman K, Endo A, et al. ICRP Publication 143: paediatric reference computational phantoms [published online ahead of print 2020/10/02]. *Ann ICRP* 2020; 49: 5–297.
49. Bolch W, Lee C, Wayson M, et al. Hybrid computational phantoms for medical dose reconstruction [published online ahead of print 2009/12/30]. *Radiat Environ Biophys* 2010; 49: 155–168.

50. Lee C, Lee C, Williams JL, et al. Whole-body voxel phantoms of paediatric patients--UF series B [published online ahead of print 2006/09/06]. *Phys Med Biol* 2006; 51: 4649–4661.
51. Lee C, Lodwick D, Hasenauer D, et al. Hybrid computational phantoms of the male and female newborn patient: NURBS-based whole-body models [published online ahead of print 20070516]. *Phys Med Biol* 2007; 52: 3309–3333.
52. Lee C, Lodwick D, Williams JL, et al. Hybrid computational phantoms of the 15-year male and female adolescent: applications to CT organ dosimetry for patients of variable morphometry [published online ahead of print 2008/07/25]. *Med Phys* 2008; 35: 2366–2382.
53. Xu XG, Taranenko V, Zhang J, et al. A boundary-representation method for designing whole-body radiation dosimetry models: pregnant females at the ends of three gestational periods--RPI-P3, -P6 and -P9 [published online ahead of print 2007/11/22]. *Phys Med Biol* 2007; 52: 7023–7044.
54. Hoseinian-Azghadi E, Rafat-Motavalli L and Miri-Hakimabad H. Development of a 9-months pregnant hybrid phantom and its internal dosimetry for thyroid agents [published online ahead of print 2014/02/12]. *J Radiat Res* 2014; 55: 730–747.
55. Rafat-Motavalli L, Miri-Hakimabad H and Hoseinian-Azghadi E. Hybrid pregnant reference phantom series based on adult female ICRP reference phantom. *Radiat Phys Chem* 2018; 144: 386–395.
56. Rafat Motavali L, Rafat Motevalli N and Miri Hakimabad SH. The first series of Iranian BREP phantoms. In: Paper presented at: 7th international workshop on computational human phantoms, 2019.
57. Kim CH, Jeong JH, Bolch WE, et al. A polygon-surface reference Korean male phantom (PSRK-man) and its direct implementation in Geant4 Monte Carlo simulation [published online ahead of print 2011/04/28]. *Phys Med Biol* 2011; 56: 3137–3161.
58. Kim CH, Yeom YS, Nguyen TT, et al. New mesh-type phantoms and their dosimetric applications, including emergencies [published online ahead of print 2018/04/14]. *Ann ICRP* 2018; 47: 45–62.
59. Kim CH, Yeom YS, Petoussi-Henss N, et al. ICRP publication 145: adult mesh-type reference computational phantoms. *Ann ICRP* 2020; 49: 13–201.
60. LaCroix K. Evaluation of an attenuation compensation method with respect to defect detection in Tc-99m-sestamibi myocardial SPECT [PhD Thesis]. *Dept. of biomedical engineering*. Chapel Hill, NC: Univ. of North Carolina, 1997.
61. Segars WP, Bond J, Frush J, et al. Population of anatomically variable 4D XCAT adult phantoms for imaging research and optimization [published online ahead of print 2013/04/06]. *Med Phys* 2013; 40: 043701.
62. Ghaly M, Du Y, Fung GS, et al. Design of a digital phantom population for myocardial perfusion SPECT imaging research [published online ahead of print 2014/05/21]. *Phys Med Biol* 2014; 59: 2935–2953.
63. Könik A, Connolly CM, Johnson KL, et al. Digital anthropomorphic phantoms of non-rigid human respiratory and voluntary body motion for investigating motion correction in emission imaging [published online ahead of print 2014/06/14]. *Phys Med Biol* 2014; 59: 3669–3682.
64. Hegenbart L, Na YH, Zhang JY, et al. A Monte Carlo study of lung counting efficiency for female workers of different breast sizes using deformable phantoms [published online ahead of print 2008/09/11]. *Phys Med Biol* 2008; 53: 5527–5538.
65. Akhavanallaf A, Xie T and Zaidi H. Development of a library of adult computational phantoms based on anthropometric indexes. *IEEE Transactions on Radiation and Plasma Medical Sciences* 2019; 3: 65–75.
66. Vazquez JA, Ding A, Haley T, et al. A dose-reconstruction study of the 1997 Sarov criticality accident using animated dosimetry techniques [published online ahead of print 2014/03/29]. *Health Phys* 2014; 106: 571–582.
67. Han B, Zhang J, Na YH, et al. Modelling and Monte Carlo organ dose calculations for workers walking on ground contaminated with Cs-137 and Co-60 gamma sources [published online ahead of print 2010/07/29]. *Radiat Prot Dosimetry* 2010; 141: 299–304.
68. Su L, Han B and Xu XG. Calculated organ equivalent doses for individuals in a sitting posture above a contaminated ground and a PET imaging room [published online ahead of print 2011/04/26]. *Radiat Prot Dosimetry* 2012; 148: 439–443.
69. Yeom YS, Han H, Choi C, et al. Posture-dependent dose coefficients of mesh-type ICRP reference computational phantoms for photon external exposures [published online ahead of print 20190404]. *Phys Med Biol* 2019; 64: 075018.
70. Johnson PB, Whalen SR, Wayson M, et al. Hybrid patient-dependent phantoms covering statistical distributions of body morphometry in the US adult and pediatric population. *Proc IEEE* 2009; 97: 2060–2075.
71. Ding A, Mille MM, Liu T, et al. Extension of RPI-adult male and female computational phantoms to obese patients and a Monte Carlo study of the effect on CT imaging dose [published online ahead of print 2012/04/07]. *Phys Med Biol* 2012; 57: 2441–2459.
72. Pi Y, Liu T and Xu XG. Development of a set of mesh-based and age-dependent Chinese phantoms and application for CT dose calculations [published online ahead of print 2018/01/18]. *Radiat Prot Dosimetry* 2018; 179: 370–382.
73. Broggio D, Beurrier J, Bremaud M, et al. Construction of an extended library of adult male 3D models: rationale and results. *Physics in Medicine & Biology* 2011; 56: 7659.
74. Lloyd B, Cherubini E, Farcito S, et al. Covering population variability: morphing of computation anatomical models. In: Paper presented at: international workshop on simulation and synthesis in medical imaging, 2016.
75. Geyer AM, O'Reilly S, Lee C, et al. The UF/NCI family of hybrid computational phantoms representing the current US population of male and female children, adolescents, and adults--application to CT dosimetry [published online ahead of print 2014/08/22]. *Phys Med Biol* 2014; 59: 5225–5242.
76. Kim JS, Ha WH, Jeong JH, et al. Use of photographic images to construct voxel phantoms for use in whole-body counting [published online ahead of print 2009/12/03]. *Radiat Prot Dosimetry* 2010; 138: 119–122.

77. Choi C, Yeom YS, Lee H, et al. Body-size-dependent phantom library constructed from ICRP mesh-type reference computational phantoms [published online ahead of print 2020/04/29]. *Phys Med Biol* 2020; 65: 125014.
78. Hoseinian Azghadi E, Miri Hakimabad SH and Rafat Motavali L. Population of whole-body statistical adult phantoms and assessing the uncertainty of organ doses in hyperthyroid treatment with 131I. In: Paper presented at: 5th international workshop on computational human phantoms, 2015.
79. Karami M, Miri-Hakimabad H, Hoseinian-Azghadi E, et al. A method for assessing subject-specific counting efficiency of whole-body monitoring systems for radioiodine measurements. *Radiat Meas* 2020; 137: 106430.
80. Rafat Motavali L and Miri Hakimabad SH. Virtual calibration of whole-body counter using a library of statistical phantoms. In: Paper presented at: 7th international workshop on computational human phantoms, 2019.
81. Erickson DW, Wells JR, Sturgeon GM, et al. Population of 224 realistic human subject-based computational breast phantoms [published online ahead of print 2016/01/10]. *Med Phys* 2016; 43: 23.
82. Kim HS, Yeom YS, Nguyen TT, et al. Inclusion of thin target and source regions in alimentary and respiratory tract systems of mesh-type ICRP adult reference phantoms [published online ahead of print 2017/01/24]. *Phys Med Biol* 2017; 62: 2132–2152.
83. Yeom YS, Kim HS, Nguyen TT, et al. New small-intestine modeling method for surface-based computational human phantoms [published online ahead of print 2016/03/24]. *J Radiol Prot* 2016; 36: 230–245.
84. Choi C, Shin B, Yeom YS, et al. Development of skeletal systems for ICRP pediatric mesh-type reference computational phantoms [published online ahead of print 20210601]. *J Radiol Prot* 2021; 41: 139–161.
85. Han H, Yeom YS, Nguyen TT, et al. Development of detailed pediatric eye models for lens dose calculations [published online ahead of print 2021/04/22]. *J Radiol Prot* 2021; 41: 45–52.
86. Abadi E, Segars WP, Sturgeon GM, et al. Modeling lung architecture in the XCAT series of phantoms: physiologically based airways, arteries and veins. *IEEE Trans Med Imaging* 2018; 37: 693–702.
87. Iacono MI, Neufeld E, Akinnagbe E, et al. MIDA: a multimodal imaging-based detailed anatomical model of the human head and neck [published online ahead of print 2015/04/23]. *PLoS One* 2015; 10: e0124126.
88. Yeom YS, Choi C, Han H, et al. Dose coefficients of mesh-type ICRP reference computational phantoms for external exposures of neutrons, protons, and helium ions. *Nucl Eng Technol* 2020; 52: 1545–1556.
89. Xie T, Akhavanallaf A and Zaidi H. Construction of patient-specific computational models for organ dose estimation in radiological imaging [published online ahead of print 20190322]. *Med Phys* 2019; 46: 2403–2411.
90. Carter LM, Camilo Ocampo Ramos J, Bolch WE, et al. Technical note: patient-morphed mesh-type phantoms to support personalized nuclear medicine dosimetry – a proof of concept study [published online ahead of print 2021/02/18]. *Med Phys* 2021; 48: 2018–2026.
91. Fu W, Sharma S, Abadi E, et al. Iphantom: a framework for automated creation of individualized computational phantoms and its application to CT organ dosimetry [published online ahead of print 20210805]. *IEEE J Biomed Health Inform* 2021; 25: 3061–3072.
92. Peng Z, Fang X, Yan P, et al. A method of rapid quantification of patient-specific organ doses for CT using deep-learning-based multi-organ segmentation and GPU-accelerated Monte Carlo dose computing [published online ahead of print 20200403]. *Med Phys* 2020; 47: 2526–2536.
93. Gibson E, Giganti F, Hu Y, et al. Automatic multi-organ segmentation on abdominal CT with dense V-networks [published online ahead of print 20180214]. *IEEE Trans Med Imaging* 2018; 37: 1822–1834.
94. Nazari M, Jimenez-Franco LD, Schroeder M, et al. Automated and robust organ segmentation for 3D-based internal dose calculation [published online ahead of print 20210607]. *EJNMMI Res* 2021; 11: 53.
95. Arabi H, AkhavanAllaf A, Sanaat A, et al. The promise of artificial intelligence and deep learning in PET and SPECT imaging [published online ahead of print 2021/03/26]. *Phys Med* 2021; 83: 122–137.
96. Fu Y, Lei Y, Wang T, et al. Deep learning in medical image registration: a review [published online ahead of print 20201022]. *Phys Med Biol* 2020; 65: 20TR01.
97. Chen J, Li Y, Du Y, et al. Generating anthropomorphic phantoms using fully unsupervised deformable image registration with convolutional neural networks [published online ahead of print 20201109]. *Med Phys* 2020; 47: 6366–6380.
98. Bauer DF, Russ T, Waldkirch BI, et al. Generation of annotated multimodal ground truth datasets for abdominal medical image registration [published online ahead of print 20210502]. *Int J Comput Assist Radiol Surg* 2021; 16: 1277–1285.
99. Xie T and Zaidi H. Estimation of the radiation dose in pregnancy: an automated patient-specific model using convolutional neural networks [published online ahead of print 20190621]. *Eur Radiol* 2019; 29: 6805–6815.
100. Zhang Y, Miao S, Mansi T, et al. Unsupervised X-ray image segmentation with task driven generative adversarial networks [published online ahead of print 20200207]. *Med Image Anal* 2020; 62: 101664.